

2015

Tp53 and Hras Influence on HPV16 E7 Expression in HPV16-Transformed Human Keratinocytes

Nella Christie Delva

University of South Carolina - Columbia

Follow this and additional works at: <https://scholarcommons.sc.edu/etd>



Part of the [Biology Commons](#)

Recommended Citation

Delva, N. C.(2015). *Tp53 and Hras Influence on HPV16 E7 Expression in HPV16-Transformed Human Keratinocytes*. (Master's thesis). Retrieved from <https://scholarcommons.sc.edu/etd/3090>

This Open Access Thesis is brought to you by Scholar Commons. It has been accepted for inclusion in Theses and Dissertations by an authorized administrator of Scholar Commons. For more information, please contact dillarda@mailbox.sc.edu.

**Tp53 and Hras Influence on HPV16 E7 Expression in HPV16-
Transformed Human Keratinocytes**

by

Nella Christie Delva

Bachelor of Science
Barry University, 2012

Submitted in Partial Fulfillment of the Requirements

For the Degree of Master of Science in

Biological Sciences

College of Arts and Sciences

University of South Carolina

2015

Accepted by:

Lucia Pirisi-Creek, Director of Thesis

Bert Ely, Reader

David Reisman, Reader

Lacy Ford, Vice Provost and Dean of Graduate Studies

©Copyright by Nella Christie Delva, 2015
All Rights Reserved.

DEDICATION

This thesis is dedicated to my parents who will always be my #1 supporter.

ACKNOWLEDGMENTS

First and foremost I'd like to thank GOD for giving me the courage and determination to stay and continue with this journey. Secondly, I'd like to thank my Mentor and PI, Dr Bert Ely and Dr Lucia Pirisi-Creek, respectively. This journey hasn't been easy and it wouldn't have been possible if I didn't have such amazing mentoring and support. I would also like to acknowledge my beautiful family for being my biggest supporter, especially my sister who has been there with me through the ups and downs.

Last but not least, thank you to my lab members who guided me through my research project Maria Hosseinipour, Yvon Woappi, Christian Graves and Fadi Abboodi. I also want to thank Ariana Renrich with whom I started this project. I am very grateful to have been a member of this amazing lab-crew.

“The difference between a successful person and others is not a lack of strength, not a lack of knowledge, but rather a lack of will.”

By Vince Lombardi

ABSTRACT

Head and Neck Squamous Carcinoma (HNSCC) is one of the most common cancers worldwide. HNSCC affects regions of the upper aerodigestive tract such as the lip, tongue, nasopharynx, oropharynx, larynx, and hypopharynx. About 25% of all HNSCC cases and up to 65% of Oropharyngeal Carcinoma (OPC) cases are positive for HPV DNA. African American patients, especially males, present primarily with HPV-negative HNSCC. HNSCC's that are HPV-positive tend to be HPV-active at initial presentation: these cancers contain HPV DNA and express HPV RNA. However, recurring HPV-positive cancers of the head and neck are more often inactive: these tumors contain HPV DNA, but do not express viral mRNA. Previous gene expression profiling results identify a gene expression signature of **HPV-inactive tumors** that is “intermediate” between HPV-active and HPV-negative cancers. This study focuses on the molecular characteristics of HPV-inactive tumors and the molecular mechanisms by which these tumors may lose E6 and E7 oncogene expression. E6 and E7 are viral oncogenes whose expression drives cells to proliferate indefinitely and lose sensitivity to senescence and growth arrest mechanisms (immortalization). Our hypothesis is that tumors that are HPV-inactive began as HPV-active lesions, where tumor cells lost expression of E6/E7 by either mutation or epigenetic mechanisms or both. In these tumors, the growth promoting effects of E6/E7 should be replaced by mutations of relevant key genes. This project is aimed towards uncovering specific *molecular*

mechanisms by which HPV-transformed cells can escape the need for continuous E6/E7 expression for proliferation. In order to explore our hypothesis, we have developed two specific aims: 1) to determine whether mutated H-Ras (H-RasV12) expression results in changes in E7 mRNA and Rb protein levels in HKc. Our results indicate that H-RasV12 partially replaces E7 function. 2) To determine whether p53 knock-down by the means of an shRNA can be achieved in Human Keratinocyte lines transformed with HPV16 (HKc/HPV16) and their respective HKc/DR cells lines, and to assess the effect of p53 knock-down on the response of HKc/HPV16 to UV.

TABLE OF CONTENTS

Dedication	iii
Acknowledgements	iv
Abstract	v
List of figures	ix
List of abbreviations	x
Chapter 1: Introduction	1
1.1. Head and neck cell carcinoma	1
1.2. Human Papillomavirus (HPV)	3
1.3. P53 and RB pathway in HPV-mediated carcinogenesis	6
1.4. Rational and Hypothesis	9
1.5. Aims	13
1.6. Broader Impact	13
Chapter 2: Materials and Methods	14
2.1. Cell culture	14
2.2. Skin processing	14
2.3. Transforming competent cells	16
2.4. Making Lb agar plates	17
2.5. Cloning p53 shRNA	17
2.6. Gel purification	18

2.7. Transfection	19
2.8. Puromycin selection.....	20
2.9. UV treatment	20
2.10. Gel Collection and Protein extraction.....	21
2.11. Bradford Assay	21
2.12. Elisa (PathScan® Sandwich ELISA Kit).....	22
2.13. RNA extraction	22
2.14. cDNA Synthesis (iScript Kit)	23
2.15. Real time PCR.....	24
Chapter 3: Results	25
3.1. Preliminary work	25
3.2. Aim 1	31
3.3. Aim 2	34
Chapter 4: Discussion	44
References.....	47

LIST OF FIGURES

Figure 1.1, Head and neck cancer regions	1
Figure 1.2 Papilloma virus life cycle	5
Figure 1.3, Mechanisms of oncogene activation: point mutation; the Ras story	8
Figure 1.4, Results of genes ontology analysis of microarray	10
Figure 1.5, Possible mechanisms for the acquisition of independence from E6/E7	12
Figure 2.6, In vitro model of HPV16-mediated carcinogenesis	16
Figure 3.7. Hairpin structure schematic	26
Figure 3.8, pSuper.retro puro map	27
Figure 3.9, Purification of digested plasmid DNA (pSuper.retro puro)	28
Figure 3.10, pBabe puro HrasV12 map	29
Figure 3.11, DNA extraction Gel.....	30
Figure 3.12: RT/q-PCR results for E7 levels HKc16/D-1++ HRas transfected cell line...	32
Figure 3.13, ELISA Rb levels in HKc/HPV16d-1 cells transfected with HRas.....	33
Figure 3.14, p53 ELISA results in normal HKc	35
Figure 3.15, p53 ELISA results in HKc/HPV16 non-transfected UV treated cells.....	36
Figure 3.16. p53 ELISA results in HKc/HPV16 non-transfected UV treated cells.....	37
Figure 3.17, Tp53 ELISA results in the HKc/HPV16d-1 cell line (D1++)	39
Figure 3.18, UV treated HKc/HPV16 cell morphology	40
Figure 3.19, HKc/DR Similar to our HKc/HPV16 p53i-sh transfected cells line	41

Figure 3.20, UV treated HKc/DR cell morphology	42
Figure 3.21, ELISA p53 levels in HKc/HPV16d-1 cells transfected with HRas	45

LIST OF ABBREVIATIONS

BPE	bovine pituitary extract
cDNA	complementary DNA
CM	complete medium
DNA	deoxyribonucleic acid
DR	differentiation resistant keratinocytes
EGF	epidermal growth factor
HKc	Human keratinocytes
HKc/DR	differentiation resistant, HPV16-transformed human keratinocytes
HKc/HPV16	human keratinocytes immortalized with HPV16 DNA
HKc/HPV16d-1	human keratinocytes from donor 1 immortalized with HPV16 DNA
HNSCC	head and neck squamous Carcinoma
HPV	Human papillomavirus
H-Ras	Harvey Ras
L1, L2	late open reading frames of papillomavirus
P53i	pSuper.p53
PBS	phosphate buffered saline
PCR	polymerase chain reaction
PV	papillomavirus
Rb	retinoblastoma protein

RT-PCR..... real time polymerase chain reaction

URRupstream regulatory region

UV light Ultraviolet light

CHAPTER 1: INTRODUCTION

1.1 Head and neck cell carcinoma

Head and Neck Squamous Carcinoma (HNSCC) is the 6th most common cancer worldwide. HNSCC begins in the squamous cells that line the moist surfaces inside the head and neck (1); it affects regions of the upper aerodigestive tract such as the lip, tongue, nasopharynx, oropharynx, larynx, and hypopharynx. Nearly 50,000 new cases of HNSCC are diagnosed in the United States every year, and there are around 10,000 deaths annually; it accounts for ~4% of all malignancies worldwide and 5% mortality of all cancers (1).

The important risk factors associated with HNSCC include tobacco use, alcohol use (1, 2), human papillomavirus infection (HPV) and Epstein-Barr virus (EBV) (3). The incidence of HPV-negative HNSCC, which is mostly associated with smoking and alcohol consumption, has decreased by about 50% in the last 30 years, while the incidence of HPV-associated HNSCC has increased by a concerning 225% (4,5). It was also shown that HPV-associated head and neck cancers had better prognosis and responded better to standard of care therapies (6,7).

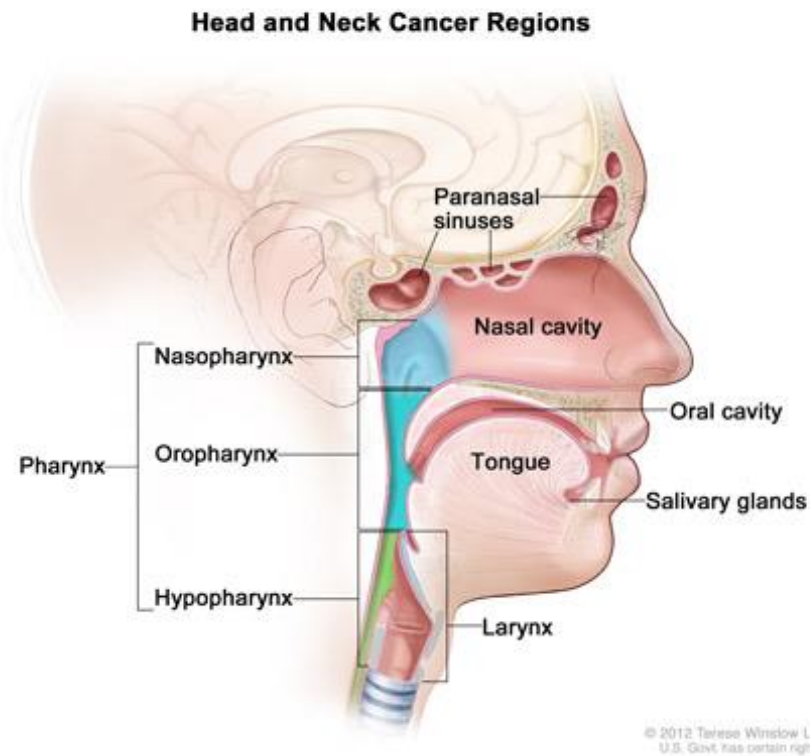


Figure 1.1. Head and neck cancer regions. The location of paranasal sinuses, nasal cavity, oral cavity, tongue, salivary glands, larynx and pharynx (including oropharynx, hypopharynx and nasopharynx) is shown.
<http://www.cancer.gov/cancertopics/factsheet/Sites-Types/head-and-neck>

1.2 Human Papillomavirus (HPV)

Papillomaviruses (PVs) are members of the *Papillomaviridae* family (8). PVs have small circular double stranded DNA genomes of approximately 8000 base pairs and icosahedral capsids (9). PVs have a unique characteristic of well-adapting biological behavior in a specific host, for example HPV virus follows the differentiation programming of its host keratinocytes (reference). PVs are in both humans and animals and can be transmitted only through close cutaneous contact with infected exfoliated skin cells or muco-mucosal contact (10). PV genomes encode five proteins and are divided into three main regions: 1) the noncoding upstream regulatory regions (URR) which regulates viral gene expression. 2) The early region (E1, E2, E4, E5, E6, and E7) is critical for virus replication, oncogenesis and survival; E1 and E2 influence the replication cycle and transcription while the E4 protein contributes to the genome amplification efficiency. E5, E6 and E7 proteins maintain a key role in cellular growth regulation. 3) The late region (structural L1 and L2) encodes viral capsid proteins. This late region contains the L1 opening reading frame (ORF) and also is the most conserved amongst all papilloma virus types (10).

1.2.1 HPV infection

Although HPV infections are mostly subclinical, some of those subclinical infections can become clinical and may develop into tumors (11). The process of HPV infection is slow. It spreads through epithelial tissue through micro-abrasions, followed

by expression of early response genes (E1, E2, E4, E5, E6 and E7). The expression of these genes allows viral genome replication. Replication then moves to the upper cell layer and starts to differentiate (11). The expression of late genes, L1 and L2, as well as E4, is followed. L1 and L2 encapsidate the viral genomes to form progeny virions in the nucleus. The shed virus can then initiate a new infection, which in turn can cause HPV lesions arisen from the proliferation of infected basal keratinocytes. In addition, Low-grade intraepithelial lesions support productive viral replication (12).

Human papillomavirus (HPV) is the most common sexually transmitted infection (15). When HPV infection persists, it can produce precancerous lesions that may develop into invasive cancers. HPV has been found to be associated with many types of cancer including: cervical, vulvar, vaginal, penile, anal, and oropharyngeal (back of the throat, including the base of the tongue and tonsils). Although there are over 200 types of HPV that have been identified only 40 types are oncogenic (13,16), HPV16 is one of the most causative agents leading to invasive cancers, it was also found be associated with HNSCC (13,14).

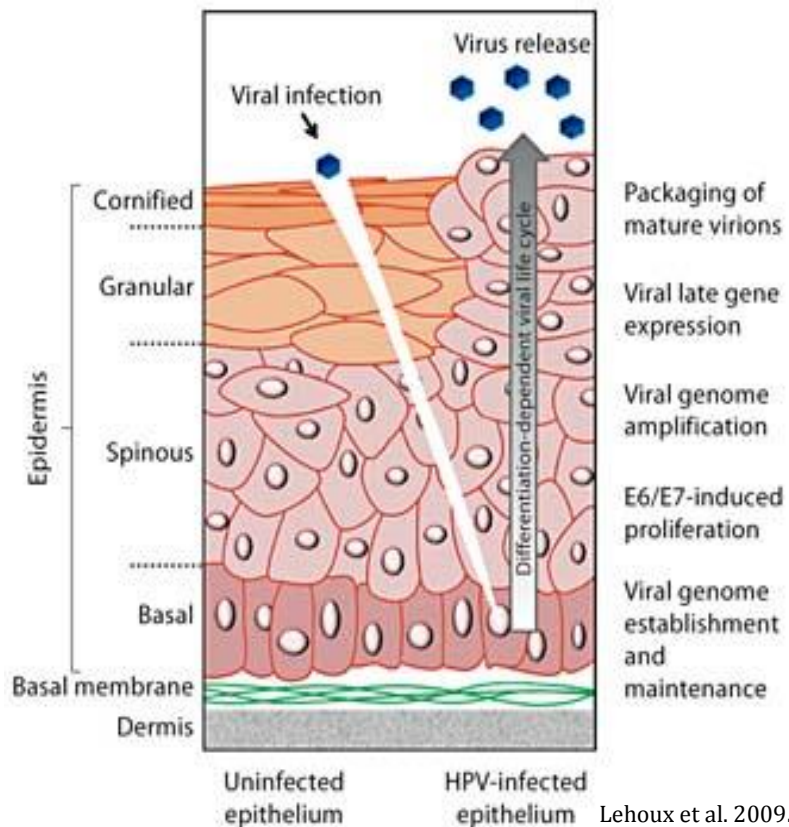


Figure 1.2 Papilloma virus life cycle HPV virus infects the basal epithelial cells through small lesion in the tissue, at this point the virus has minimal DNA replication and viral gene expression in basal cells (maintenance replication). Viral gene expression begins in the suprabasal cells, which induces proliferation due to E6 and E7, this process is followed by viral genome amplification. Late genes expression at the upper layers of the infected epithelium and lastly, virus assembly occurs in the most differentiated upper layers, then release.

1.3 P53 and RB pathway in HPV16-mediated carcinogenesis

Tp53 is tumor suppressor gene that plays an important role in cell cycle and apoptosis. It is also called the “guardian” of the genome. The p53 protein transactivates a number of proteins with functions in cell cycle arrest and apoptosis (17). On the other hand, the tumor suppressor protein retinoblastoma (pRb) controls the expression of genes involved in cell cycle progression (18). These two tumor suppressor genes were found to have strong association with various type of cancer including HNSCC.

In the case of HPV16-mediated carcinogenesis, the tumors are driven by the E6 and E7 viral oncoproteins (19, 20). E6 and E7 are viral oncogenes whose expression drives cells to proliferate indefinitely and lose sensitivity to senescence and growth arrest mechanisms (immortalization) (20, 21). E6 binds and degrades the p53 protein (22, 25), causing the cells to continue proliferating even in the presence of stressors or DNA damage. E7 disrupts the interaction between Rb and E2F and promotes the degradation of Rb. E7-mediated degradation of Rb frees up E2F to stimulate DNA replication and eventually cell division (23, 24, 26). Therefore, HPV hijacks cell cycle regulatory pathways and allows cells with damaged DNA to continue to grow and replicate. Mutations of p53 and Rb pathways alone can increase replication potential and cause immortalization (28). A number of studies have shown that different cancers showed the presence of p53 mutations (69.8% of HNSCC) (29) however, in HPV-mediated cancers, p53 function is just deactivated by E6 and mutations of p53 are rare. p53 function can also be inactivated by other mechanisms such as overexpression or amplification of MDM2 and deletion of the p14^{ARF} gene (29), loss of p16^{INK4A} and overexpression of

cyclin D1 associated with reduced survival (29). pRb can also be inactivated through the inactivation of the tumor-suppressive CDKN2A gene (targeted earlier in the HNSCC carcinogenesis). pRb mutations, however, are not very common in HNSCC, with about 7-9% mutation and copy number losses in 20–30% of cases (32). Instead, the H-RAS gene is significantly mutated in head and neck squamous cell carcinomas (HNC) and is a putative oncogenic driver (34). Oncogenic *Ras* mutations cause the protein to be perpetually active in the GTP-bound state resulting in increased proliferation and survival signaling (34). When looking at all human cancers, *KRas* mutations (part of the Ras family) are the most common type of *Ras* mutation (34), *HRas* being the least common. In addition, Oncogenic *HRas* mutations have been specifically found on codons 12, 13, 61. Conversely, in HNSCC, *Ras* mutations appear to be exclusively *H-Ras* mutations (35).

1.4 Rationales and Hypothesis

Previous studies indicated that African American (AA) patients develop HPV-negative Head and Neck Squamous Carcinomas (HNSCCs) more frequently than do European American (EA) patients (36, 37). It was also found that HPV in AA HNSCC patients is most often inactive, meaning that the tumors are positive for viral genomic DNA, but they do not express transcripts encoding E6 and E7 oncoproteins (37). About 25% of all HNSCC cases, and up to 65% of Oropharyngeal Carcinoma (OPC) cases are positive for HPV DNA. African American patients, especially males, present primarily with HPV-negative HNSCC, and we have found that those that are HPV-positive by DNA are most often HPV-inactive (36, 37).

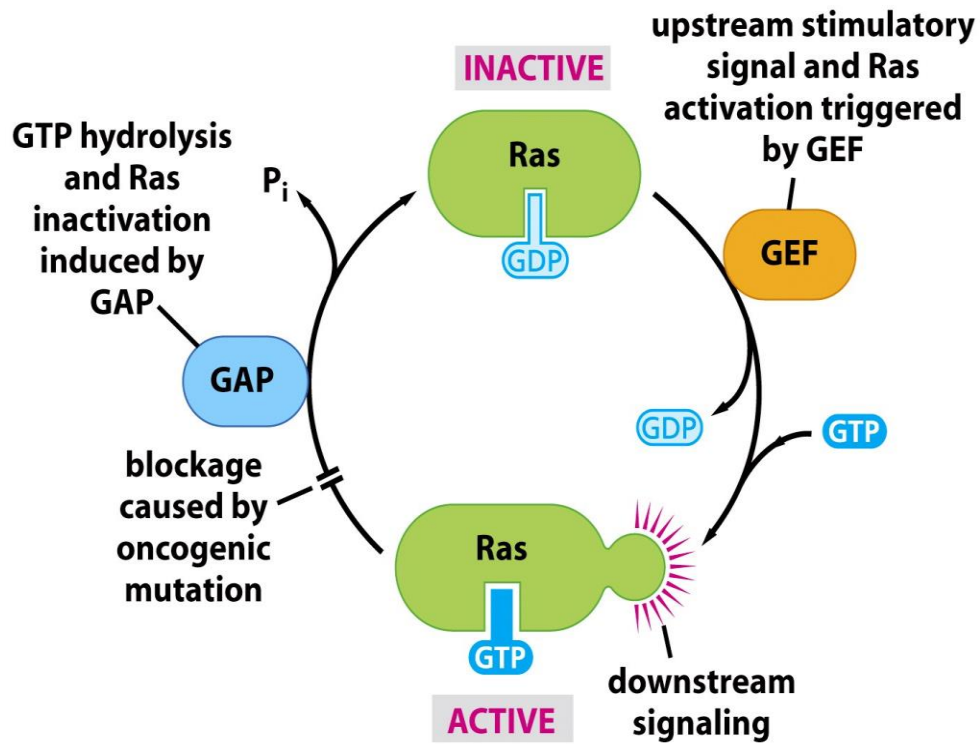


Figure 1.3: Mechanisms of oncogene activation: point mutation the Ras story
 When *Ras* is mutated, *Ras* becomes “stuck” in the “on” (GTP-bound) position and cells are constantly replicating.

HNSCC's that are HPV-positive tend to be HPV-active at initial presentation, whereas HPV-positive recurring cancers of the head and neck are more often inactive (36). Previous gene expression profiling results identify a gene expression signature of HPV-inactive tumors that is an "intermediate" between HPV-active, positive for viral DNA and expressing E6 and E7 transcripts and HPV-negative cancers where viral DNA is not present nor express E6 and E7 (36,37). The gene oncology analysis below (a former graduate student project) clearly shows that HPV-inactive tumors lack the cell cycle/mitosis/proliferation signature typical of HPV-active tumors. HPV-inactive tumors share many but not all the features of HPV-negative tumors, lacking changes in a whole class of pathways including cell projections, leading edge, adherens junctions. This difference supports our statement that the signature of HPV-inactive tumors is intermediate between that of HPV-active and HPV-negative.

Our hypothesis is that tumors that are HPV-inactive began as HPV-active lesions, where tumor cells lost expression of E6/E7 by either mutation or epigenetic mechanisms or both. In these tumors, the growth promoting effects of E6/E7 should be replaced by mutations of relevant key genes. For example, E6 function could be replaced by homozygous deletion or mutation of p53; E7 function could be replaced by active ras. This project aims at uncovering specific *molecular mechanisms by which HPV-transformed cells can escape the need for continuous E6/E7 expression* for proliferation.

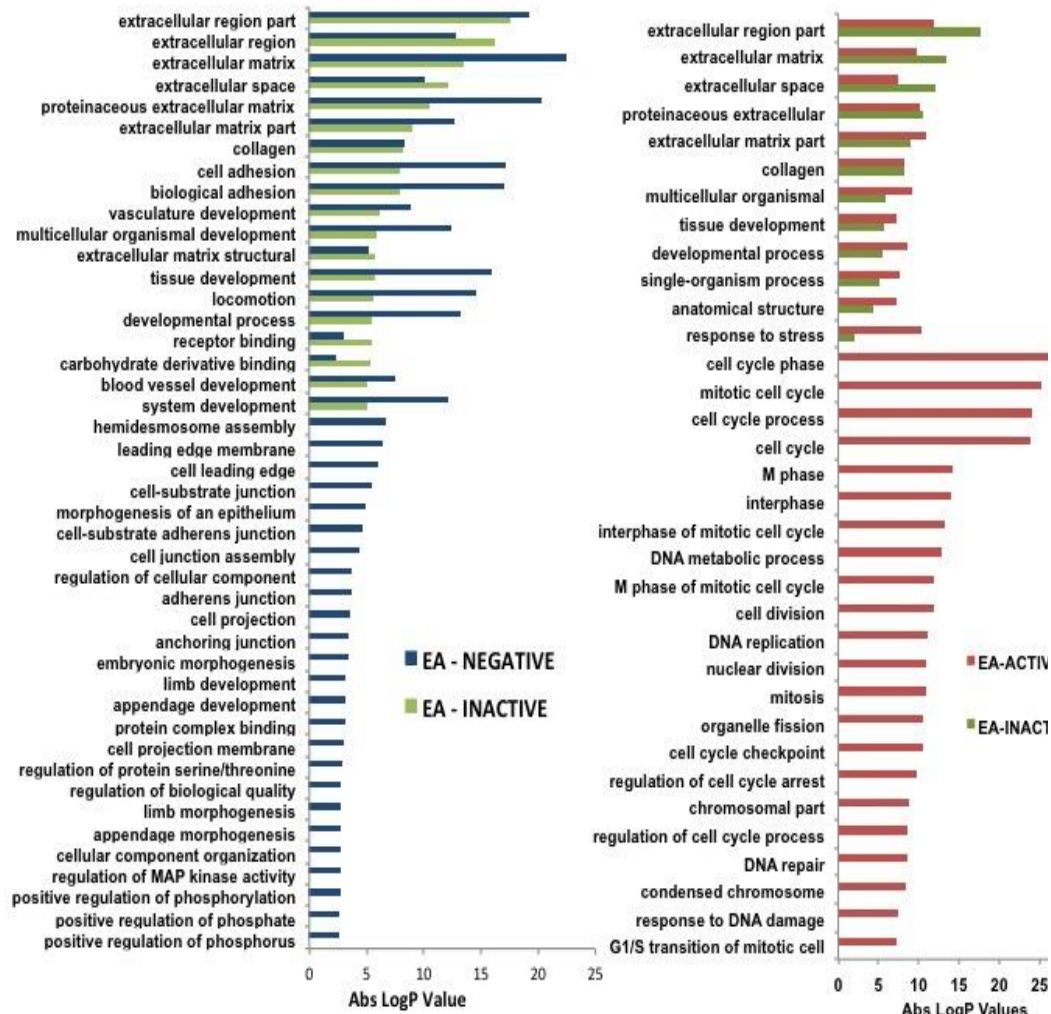


Figure 1.4. Results of gene ontology analysis of microarray results from HPV-active, HPV-inactive and HPV-negative OPC from European American patients (due to the small numbers of HPV-active, AA samples) (37)

Since HPV-inactive tumors were found to have very distinct gene expression signatures from those of HPV-positive and HPV-negative tumors, this project is exploring TP53 and H-Ras mutation profiles of HNSCC in HPV inactive patients in order to determine their clinical and genetic characteristics. *Characterizing the molecular profile of HPV-positive inactive tumors can greatly improve our understanding of the growth and progression of HPV16-mediated HNSCCs.*

This study focuses on the molecular characteristics of HPV-inactive tumors and the molecular mechanisms by which these tumors may lose E6 and E7 oncogene expression (figure 4). We reason that in cancer cells, E6 function could be replaced by homozygous deletion or mutation of p53; and E7 function could be replaced by active ras. Part of our efforts will be to show that these changes often occur in cultured HPV16-transformed cells, to provide proof of principle for this concept. We will also study HNSCC samples to determine whether mutations of p53 and/or Ras are more frequent in HPV-inactive tumors. These mutations are extremely rare in HPV active HNSCC.

1.5 Aims

Based on the above hypothesis, we have developed the 2 specific aims. First, to determine whether mutated H-Ras (H-RasV12) expression results in changes in E7 and Rb expression levels in different HKc/HPV16. Second, To determine whether p53 can be knock-down by the means of an shRNA out Human Keratinocyte lines transformed with HPV16 (HKc/HPV16) and HKc/DR lines. These studies are meant to provide justification for a comprehensive mutation analysis of HNSCC specimens that will allow us to determine which mutations are associated with the HPV-inactive group, in comparison with HPV-active and HPV-negative cancers.

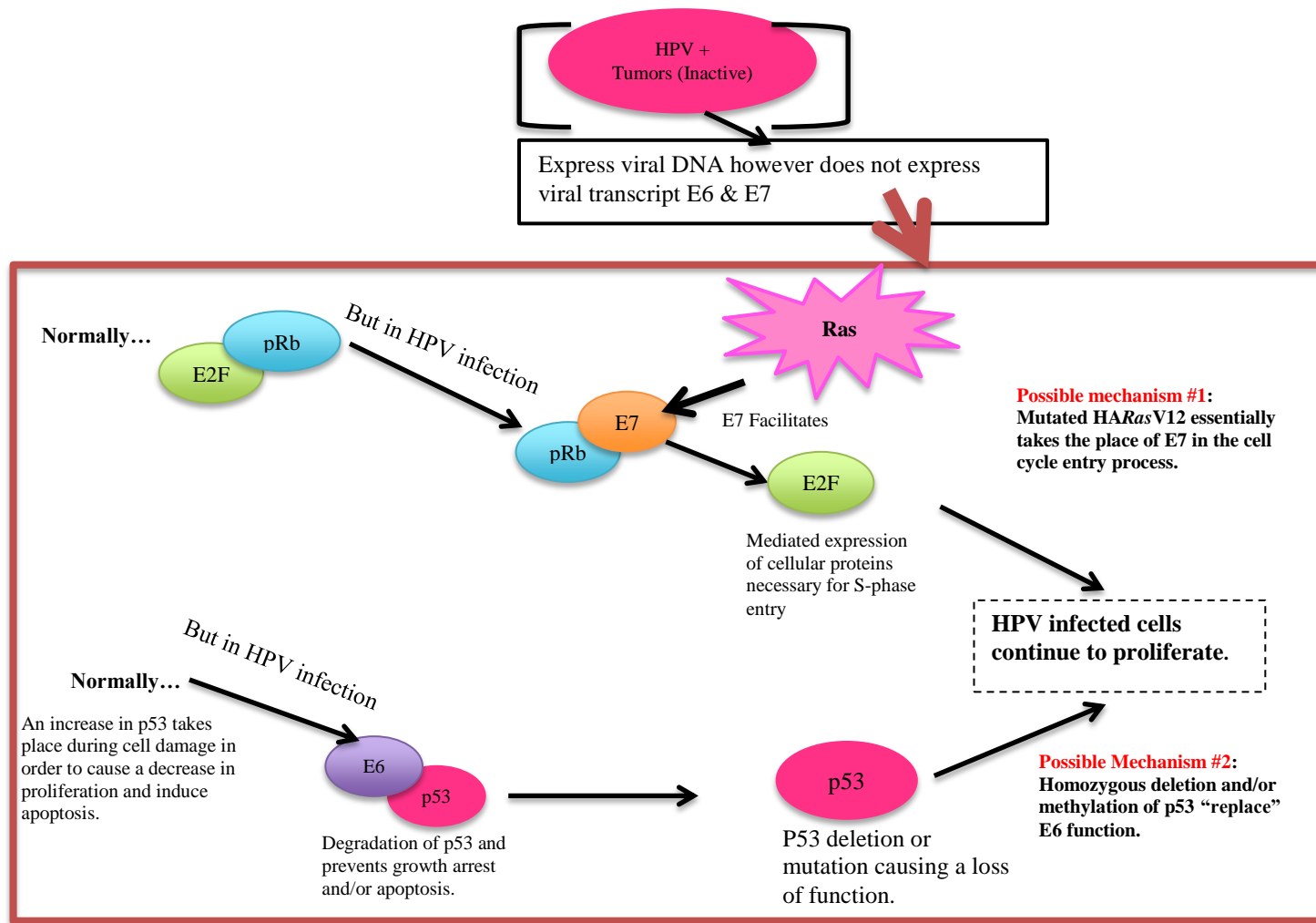


Figure 1.5 Possible mechanisms for the acquisition of independence from E6/E7 by HNC cells.

1.6 Broader Impacts

The discovery that HPV-inactive HNSCC arise as HPV-active lesions, if confirmed by *in vitro* and *ex vivo* studies, would show that HPV-inactive cancers constitute a molecular and pathogenetic group of their own, distinct not only from HPV-active but also from HPV-negative tumors. If HPV-inactive cancers begin as HPV-active, these cancers may be amenable to prevention with the HPV vaccines. In addition, there is a large body of controversial literature about the possible role of HPV in other cancers, such as the breast, the esophagus and the lung (to name a few). Currently, HPV DNA found in these tumors is interpreted as a mere passenger without a role in the development of those cancers. However if HPV-transformed cells can be mutated in such a way as to become independent of E6/E7 in the head and neck, perhaps the same mechanisms may operate at other sites. Therefore, these findings would lead to a complete revision of the role of HPV (and the potential preventive value of HPV vaccines) at other cancer sites.

CHAPTER 2: MATERIALS AND METHODS

2.1 Cell culture

The HKc/HPV16d-1 (Pirisi et al., 1987) transformed cell line was used throughout this project. Cells were taken out of the liquid nitrogen container and plated on 100-mm tissue culture plate with Keratinocyte Serum Free media (KSFM). The plate was placed in incubator (37 degrees Celsius). After plating, cells were fed the following day and wash every 48 hours until 80% confluence. Cells were again allowed to grow once more to 80% confluence before transfection, UV treatment or protein extraction.

2.2 Foreskin processing

Normal HKc cells were isolated from neonatal foreskins using the following protocol. Foreskins were rinsed under sterile conditions in a wash vial containing MCDB153-LB (home made medium) basal media. Excess connective tissue and fat were removed from the dermis using a scalpel. Foreskins were incubated overnight in incubator (37 degrees Celsius) dermis side down, in 10% dispase. The epidermis was separated from the dermis with a pair of forceps in a 100 mm Petri dish. The epidermis was then trypsonized, spun down and plated in a 100 mm cell culture dish using in 5 ml of complete medium. Cells were collected by centrifugation in a clinical centrifuge, speed 3 for 1 minute and speed 2 for 4 minutes. Cells pellet was re-suspended and plated onto a 100-mm cell culture dish in 10ml of CM. The next day, the cell were washed with

PBS and fed once more with 15 ml of CM then incubated in a humidified atmosphere of 95%air/5%CO₂. Cells were fed fresh CM every 48 hour until cells reached 80% confluence.

In order to knock-down p53 and overexpress H-Ras in the HPV16-transformed cell lines the following procedures were performed:

2.3 Transforming competent cells

The following materials were prepared: Water bath was equilibrated to 42 degrees Celsius, S.O.C medium and LB medium were warmed to room temperature, and Selective plates (100ug/ml ampicillin in LB Agar) were warmed in a 37 degree incubator for 30 minutes.

One vial of Shot TOP10 (Invitrogen) chemically competent cells for each transformation was allowed to thaw on ice. 100 ng of DNA was added into a vial of One Shot cells and mixed gently. The vials were then incubated on ice for 30 minutes. The cells were heat-shocked for 30 seconds at 42 degree Celsius, and then put back on ice for 2 minutes. 250 ul of pre-warmed S.O.C medium was added to each vial. The vial was capped tightly and shaken horizontally at 37 degree Celsius for 1 hour at 225 rpm in a shaking incubator. 200 ul from each transformation was spread a pre-warmed selective plate and incubated overnight at 37 degrees Celsius.

Model System of HPV-Mediated Carcinogenesis

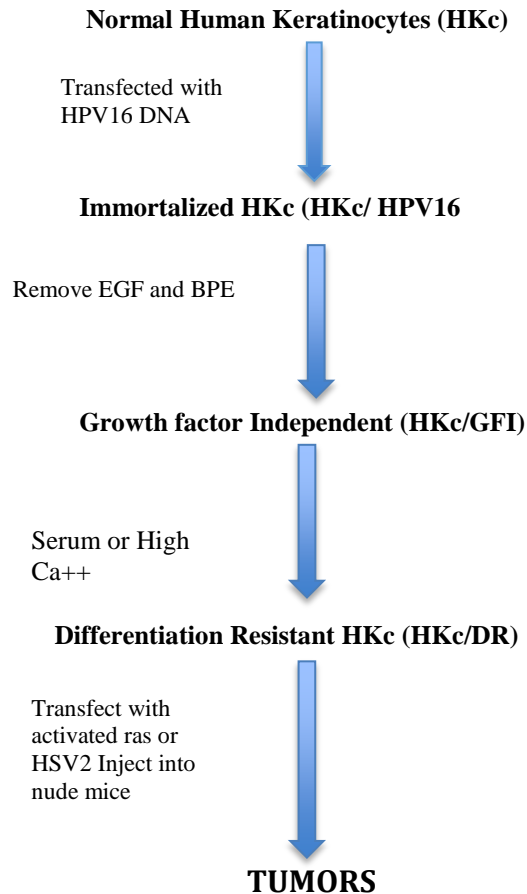


Figure 2.6. In Vitro model of HPV16-Mediated Carcinogenesis. HKc cells are isolated from neonatal foreskins transfected with HPV16 plasmid DNA. HKc/HPV16 immortalized cells grew in the MCDB152-LB medium containing epidermal growth factor (EGF) and bovine pituitary extract (BPE) for proliferation. The derived HKc/GFI are selected in media containing high calcium (>0.3mM) and fetal bovine serum, giving rise to differentiation resistant cells (HKc/DR). HKc/DR when transfected with activated ras or HSV2 or SIX1 into nude mice, these HKc/DR cells developed into tumors.

2.4 Making LB agar Plates

250 mL of distilled water was measured and 25 grams of premix LB agar powder (VWR DF0445-17) was weighed and mixed well into solution. The total volume of the mix was brought to 500 mL with distilled water, and the solution was transferred to a 1L flask. This flask was put on a stirring hot plate and allowed to boil for 1 minute while stirring. The solution was transferred to 1L Pyrex jar and labeled with autoclave tape. The 1L Pyrex jar was autoclaved at liquid setting for 20 minutes. After agar had cooled down to about 55-degree Celsius, 25 ml of ampicillin (5 mg/ml) was added to the flask. Lastly, 20 ml of agar+amp was added to each 100 mm plates under the hood, and left to cool. The LB agar+amp plates were stored at +4 degree Celsius for later use.

2.5 Cloning p53 shRNA

P53 shRNA top strand

GATCCCCTTGGCAGCCAFACCTGCCTTTTCAAGAGAAAGGCAGTCTGGCTGCCAATTTT
TA

P53 shRNA bottom strand

AGCTTAAAAATTGGCAGCCAGACTGCCTTTTCTCTTGAAAAGGCAGTCTGGCTGCCA
AGGG

Briefly, the general steps in utilizing a pSUPER.retro vector include annealing the forward and reverse strands for the shRNA (shown above). Second, linearize the pSUPER.retro vector with the BglIII and HindIII restriction enzymes. Third, ligating the

annealed oligonucleotides into the vector; transform competent bacteria with the resulting ligation mix, selecting and amplifying colonies that contain the desired construct.

Annealing the forward and reverse strands: The oligonucleotides were dissolved in nuclease free H₂O to a concentration of 3 ug/mL. The annealing reaction was assembled by mixing 1 ul of each oligo (forward and reverse) with 48 ul of annealing of annealing buffer. This mixture was incubated at 90 degree Celsius for 4 min and at 70 degree Celsius for 10 minutes. The annealed oligonucleotide was cooled slowly to 10 degree Celsius and stored at -20 degree Celsius. Second step of *linearizing the vector (pSUPER.retro)*: 1 uL of the pSUPER.retro vector was linearized with *Bgl*III and *Hind*III restriction enzymes. The plasmid was first digested with *Hind*III overnight, followed by a second overnight digestion of *Bgl*III. The reaction was then heat inactivated, and the resulting DNA was separated by electrophoresis on a 1.1 % agarose gel. The band representing the pSuper plasmid with *Bgl*III/*Hind*III ends was purified as described below.

2.6 Gel Purification of pSuper plasmid with *Bgl*III/*Hind*III end

QIAquick Gel Extraction Kit was used to purify plasmid DNA. After digestion of plasmid DNA with *Hind*III and *Bgl*III, the resulting fragments were separated by electrophoresis on a 1.1% agarose gel, which was then stained with ethidium bromide. The DNA band was excised from the gel under long-wave UV light using a razor blade. The gel slice containing the DNA band of interest was cut into smaller pieces and placed into an Eppendorf tube. A volume of 400 ul of solution 1, equal to 3-fold the weight of the agarose sliced, was added to the agarose. The agarose was dissolved by incubation (55 degrees Celsius) for 6 minutes. 1 uL per ug of DNA of glass milk suspension

(provided in the kit) was added for collection of the plasmid DNA. The contents were shaken for 15 minutes at room temperature. After centrifugation (1,000 x g for 10 minutes) pellets were collected. Supernatant was discarded and re-suspension of pellet using NaI Followed. The sample was centrifuged once more, then the pellet was re-suspended in 1 ml of *new wash*. This solution was transferred to a clean and sterile Eppendorf tube. This washing procedure was repeated multiple times. DNA was then eluted from the glass milk by re-suspension in distilled H₂O. The suspension was centrifuged and the supernatant containing the DNA was transferred into a sterile Eppendorf tube.

Ligation into pSUPER.retro vector: The cloning reaction was assembled by adding 2 uL of the annealed oligonucleotide to 1 uL of T4 DNA ligase buffer. Followed by addition of 1 uL of the digested pSUPER.retro vector, 5uL nuclease-free H₂O and 1 uL T4 DNA ligase. This mixture was incubated overnight at room temperature. After cloning and prior to transformation, plasmids were treated with *Bgl*III (1ul) and incubated for 30 minutes at 37 degrees Celsius to eliminate the vector that would have re-circularized, as the *Bgl*III site was destroyed in the recombinant plasmid, but not in the re-circularized vector. The plasmid was then transformed into bacteria (*E. coli*), followed by transfection of our DNA plasmid in HKc/HPV16d-1 cells lines.

2.7 Transfection

Once the HKc/HPV16d-1 cells plated in 6-well plated reached 70-80% confluence, the Lipofectamine 3000 reagent form Promega was diluted in transfection

medium (KFSM) as recommended by the manufacturer. P53i-sh was also diluted in transfection medium. Lipofectamine 3000 and plasmid were then gently mixed (1:1 ratio). The mixture was incubated for 5 minutes. 250 μ l of this DNA-lipid complex was added to the cells and incubated for 6 hours at 37 degrees Celsius in a humidified atmosphere of 95%air/5%CO₂. Cells were then fed fresh KFSM, added to each well without removing the transfection mix.

2.8 Puromycin selection

After transfection (24hours post) , 2 mL of KFSM medium containing 3 μ g/mL of puromycin was added to each well containing transfected cells, which were then incubated for an additional 24 hours. The medium was replaced with CM media and colonies were observed closely for several days until all non-transfected cells died, and transfected cells were ready to be collected for further analysis.

2.9 UV light treatment

Cells were allowed to grow until about 70-80% confluent at 37-degree Celsius. Cells were first washed using PBS and, while the cell culture dishes were left uncovered under the hood, the UV light was turned on for a short 30 seconds. CM medium was added back to the cells and dishes were put back into the incubator at 37 degree Celsius in a humidified atmosphere of 95%air/5%CO₂ for various times (1h, 3h, 6h and 12h). After UV exposure, cells were collected for further analysis.

2.10 Cell collection and Protein extraction

CM media was aspirated when cells reached 80% confluence. After removal of media, 3 ml of 0.5 % of trypsin was added to the 100 mm dishes. The dishes were put back in the 37-degree Celsius incubator for 3 minutes or until cells were completely detached then 500 ul of FBS was added to the detached cell trypsin mixture, to inactivate the trypsin. The detached cells were then transferred to a 15 ml tube and centrifuged (in a clinical centrifuge) for minutes.

Once the cell pellets was collected, 300ul of RIPA buffer (containing protease inhibitors) was added to each tube. The samples were then incubated on ice for 5 minutes. The cell were re-suspended and lysed by vortex-ing. After transfer of mixture to a 1.5ml tube, the samples were centrifuged at 8,000x g for 10 minutes. Supernatant with cell lysate was transferred to a new tube. Protein quantification was later performed to these samples.

2.11 Bradford Assay

The standard protocol was performed in In a 250 µl microplate assay. The 1x dye reagent was removed from 4°C storage and allowed to be warmed to ambient temperature. The 1x dye reagent was inverted a few times before use. 2-mg/ml gamma-globulin standard was used. The following volumes were used 5ul of the standard in each well, 5ul of sample in each well and 190ul of 1x dye reagent in each well using disposable cuvette. Protein solutions were assayed in triplicate. For convenience, 6 different consecutive dilution of BSA was used, blank samples (0 µg/ml) was made using

water and dye reagent. The samples were mixed using a microplate mixer. The plate was incubated at room temperature for 5 min. the spectrophotometer was set to 595 nm and absorbance of the standards and samples was measured.

2.12 ELISA (PathScan[®] Sandwich ELISA Kit)

The required microwell strips were allowed to reach room temperature. Cell lysates was diluted with Sample Diluent (supplied in each PathScan[®] Sandwich ELISA Kit) to a set protein concentration. Addition of 100 µl diluted cell lysate to each well. The strips were then incubated overnight at 4°C. The strips were washed 4 times with 1X Wash Buffer using 200 µl (wash procedure) each time. After each wash, the strips were stroked on fresh towels in order to remove the residual solution in each well. 100 µl of reconstituted Detection Antibody (green color) was added to each well. The strips were incubated once more at 37°C for 1 hr. The “wash procedure” was repeated once more, followed by the Addition of 100 µl of reconstituted HRP-Linked secondary antibody to each well followed by incubation for 30 min at 37°C and “wash procedure”. After removal of reconstituted HRP-Linked secondary antibody, wells were again washed followed by the addition of 100 µl of TMB Substrate to each well. The strips were incubated for 10 min at 37°C or 30 min at 25°C, then 100 µl of STOP Solution was added to each well. Absorbance was then measured at 450 nm.

2.13 RNA Extraction

RNA was extracted using RNeasy mini kit (Qiagen) with the manufacturer's instruction. Cells were harvested, and disrupted by adding Buffer RLT. 350 µl was added

of Buffer RLT to the cell tube. The tubes were vortexed or pipetted for proper mixture. The lysates were homogenized accordingly by pipetting the lysate directly into a QIAshredder spin column placed in a 2 ml collection tube, and centrifuged for 2 min at full speed. 1 volume of 70% ethanol was added to the homogenized lysate, and mixed well by pipetting. The total volume of 700 µl of each sample was transferred from previous step, including any precipitate that may have formed. A volume of 700 µl Buffer RW1 was added to each RNeasy spin column. The flow-through is collected in the base. An additional volume of 500 µl Buffer RPE was added to each RNeasy spin column. Flow-through was again collected in the base. 500 µl Buffer RPE was added to each RNeasy spin column. The flow-through was once more collected in the base. Each column was placed in a 2 ml collection tube, centrifuged at full speed for 1 min. Each RNeasy spin column was placed in a new 1.5 ml collection tube where I added 30–50 µl RNase-free water directly to each spin column membrane. Centrifuged for 1 min at $\sim 8000 \times g$ ($\sim 10,000$ rpm) to elute the RNA. The collected RNA eluent was stored in -80 degree Celsius freezer.

2.14 cDNA Synthesis (iScript Kit)

The following items were added to a small Eppendorf tube for a total volume of 20 µl: Master mix recipe (20 µl total): 4 µl of 5x iScript reaction kit; 1 µl iScript reverse transcriptase; 4 µg/µl of RNA template and nuclease free water. The mixture was then vortexed, spun down and run cDNA was synthesized in a minicycler using iScript program. Reverse transcription was carried out in the thermocycler with the following

incubation scheme: 5 minutes at 25 degrees Celsius, 30 minutes at 42 degrees Celsius, 5 minutes at 85 degrees Celsius, with an optional hold at 4 degree Celsius. Samples was diluted with 130 ul of RNF H₂O and stored at -20 degree Celsius.

2.15 Real time PCR

cDNA was used for this Real time PCR reaction. Using iQ SYBR green supermix (Bio-Rad), 25 ul of iQ SYBR green supermix was used per sample, with varied forward and reverse primer volume and varied RNF H₂O for a total volume to 45 ul per reaction. cDNA samples were boiled for 2 minutes after 5 ul of cDNA was added to the respective wells of a 96-well Bio-Rad PCR plate along with 45 ul of master mix. Samples were run in triplicates. The plate was then sealed and centrifuged for 1 minute at 2000 rpm.

The Bio-Rad iCycler used for this PCR reaction was at 8.5 min at 95 degree Celsius followed by 50 cycles of 95 degree Celsius for 30 seconds, 55 degree Celsius for 30 seconds and 97 degree Celsius for 30 seconds. Completion of amplification with a 30 second cycle at 58 degree Celsius, 10 minutes at 72 degree Celsius and a hold at 4 degree Celsius.

CHAPTER 3: RESULTS

3.1 Preliminary work

RNA interference approach was used in order to knockdown Tp53. The pSuper.p53 vector was used, this vector includes a 19-nucleotide sequence from the target mRNA (both sense and antisense orientation), separated by a short 9-nucleotide spacer sequence, shown in the figure below.

Using the forward and reverse p53i-sh sequence, the following schematic transcript of the recombinant vector was made. This RNA product is predicted to fold back on itself to form a 19-base pair stem-loop structure.

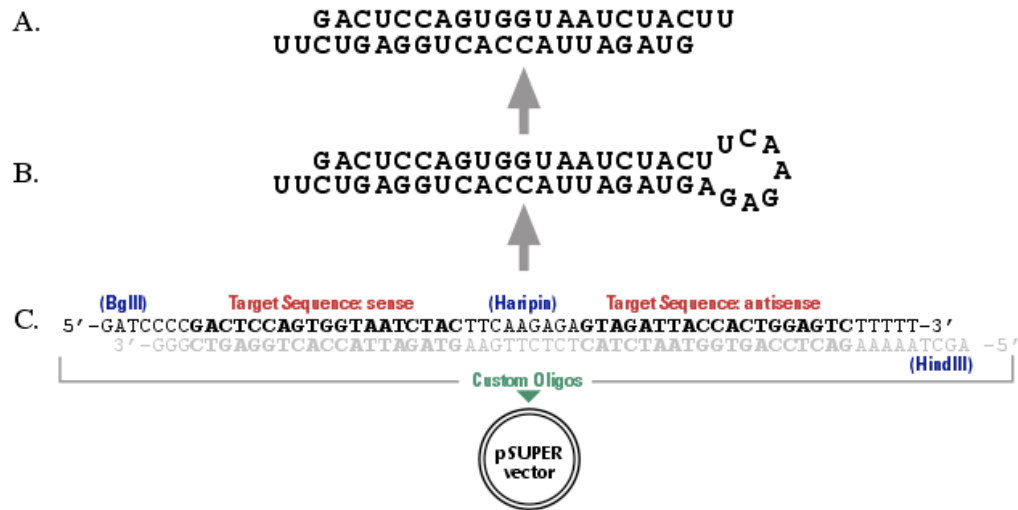


Figure 3.7. Hairpin structure schematic

Different views of the same target sequence: Fig. A shows the target sequence (sense strand) and its complement (antisense strand) in the final duplex form, each with the 3' UU overhang typical of siRNA. Fig. B shows the same sequences along with the hairpin loop, which is cleaved by the Dicer enzyme following RNA transcription. Fig. C shows the forward AND reverse 64-mer oligos (forward highlighted) in relative orientation as ligated into the pSUPER vector.

Designed sequence:

p53i-sh top strand:

GATCCCCTTGGCAGCCAGACTGCCTTTTCAAGAGAAAGGCAGTCTGGCTGCCAATTTTT

p53i-sh bottom strand:

AGCTTAAAAATTGGCAGCCAGACTGCCTTTTCTCTTGAAAAGGCAGTCTGGCTGCCAAGGG

These sequences were designed in such a way that they can form a hairpin loop structure in order to be effectively inserted into our pSUPER retro puro plasmid.

Once our DNA plasmid was ready to use, I proceeded in cloning the p53i-sh RNA into the following vector (pSuper.retro puro), following the appropriate protocol.

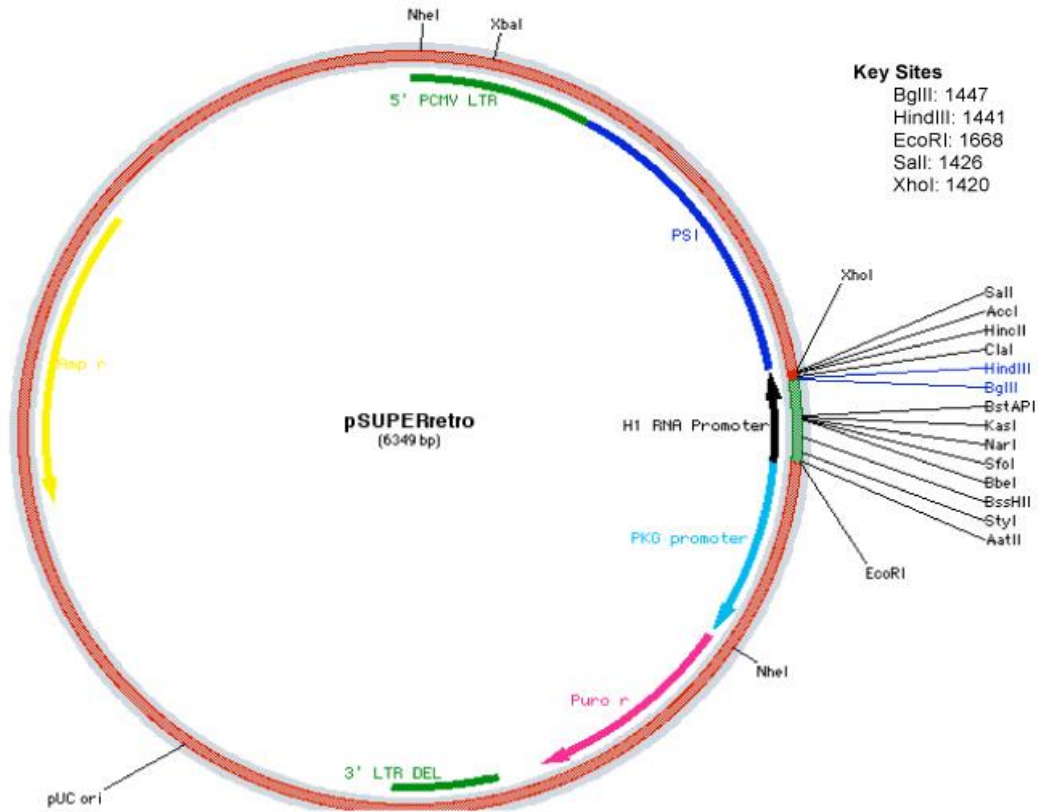


Figure 3.8 pSuper.retro puro map. PGK promoter: 2766-3164, Puro ORF: 3179-3778, H1 promoter: 2430-2650, Ampicillin resistance ORF: 6367-5501, 3' delta LTR: 3848-4201, 5' LTR: 7293-513 (homologous to other MSCV LTR), Stuffer Sequence: 1447-2423

Key Sites: *BglII*: 2424, *HindIII*: 1441, *EcoRI*: 2645, *Sall*: 1426, *XhoI*: 1420

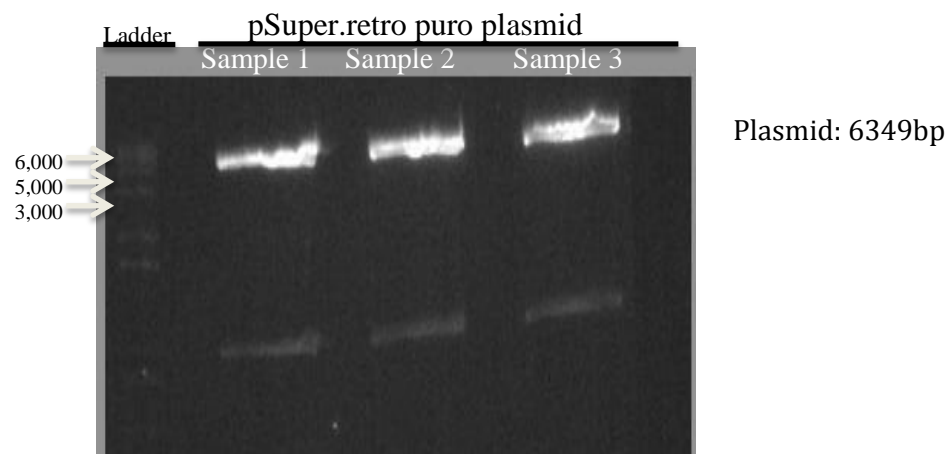


Figure 3.9. Purification of digested plasmid DNA (pSuper.retro puro) DNA plasmid was successfully digested (linearization) with HindIII and BglII (restriction enzymes). The band representing the double-cut DNA plasmid was selectively cut out of the gel and extracted for cloning.

The DNA plasmid pBabe puro H-rasV12 was ordered from *Addgene*. The DNA map of this plasmid is shown in Figure 8.



Figure 3.10. pBabe puro HrasV12 map. Mammalian Expression, Retroviral, Cloning method Restriction Enzyme: 5' cloning site BamHI (not destroyed), 3' cloning site EcoRI (not destroyed), 5' sequencing primer pBabe-5. 3' sequencing primer pBabe-3. Bacterial Resistance: Ampicillin, Growth Temperature: 37°C, Growth Strain: DH5alpha, High Copy number.

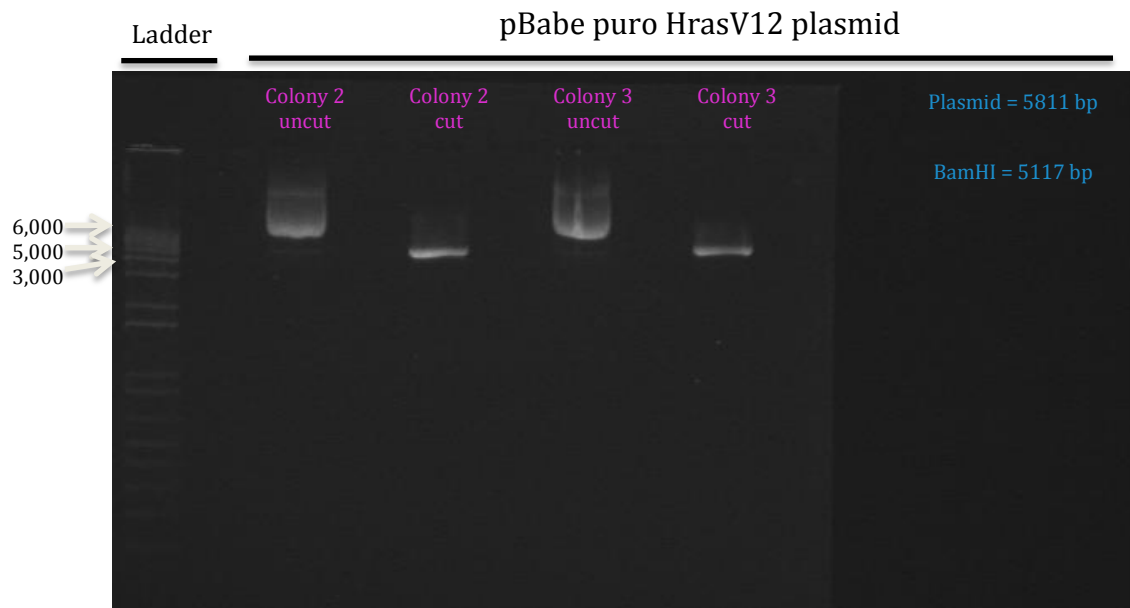


Figure 3.11. DNA extraction Gel.

Gel confirms successful presence and digestion of pBabe puro HrasV12 DNA plasmid.

3.2 Aim 1

To determine whether mutated H-Ras (H-RasV12) expression results in changes in E7 and Rb expression levels in different HKc/HPV16 and HKc/DR lines different assay was performed to measure Rb and E7 protein levels.

HKc/HPV16d-1 cells were transfected with mutated H-Ras, then RNA and protein were collected for RT/PCR for E7 and ELISA for Rb, assays using HKc/HPV16d-1 non-transfected as controls. We observed a significant decrease in E7 mRNA expression in the H-RasV12 transfected HKc/HPV16d-1 cells as compared to the non-transfected cells lines (Figure 12). As expected, this decrease in E7 expression was accompanied by a marked increase in Rb protein levels detected by ELISA in cell lysates from H-rasV12-expressing HKc/HPV16d-1, compared to their controls (Figure 13), indicating that the decrease in E7 mRNA corresponds to a decrease in active E7 protein.

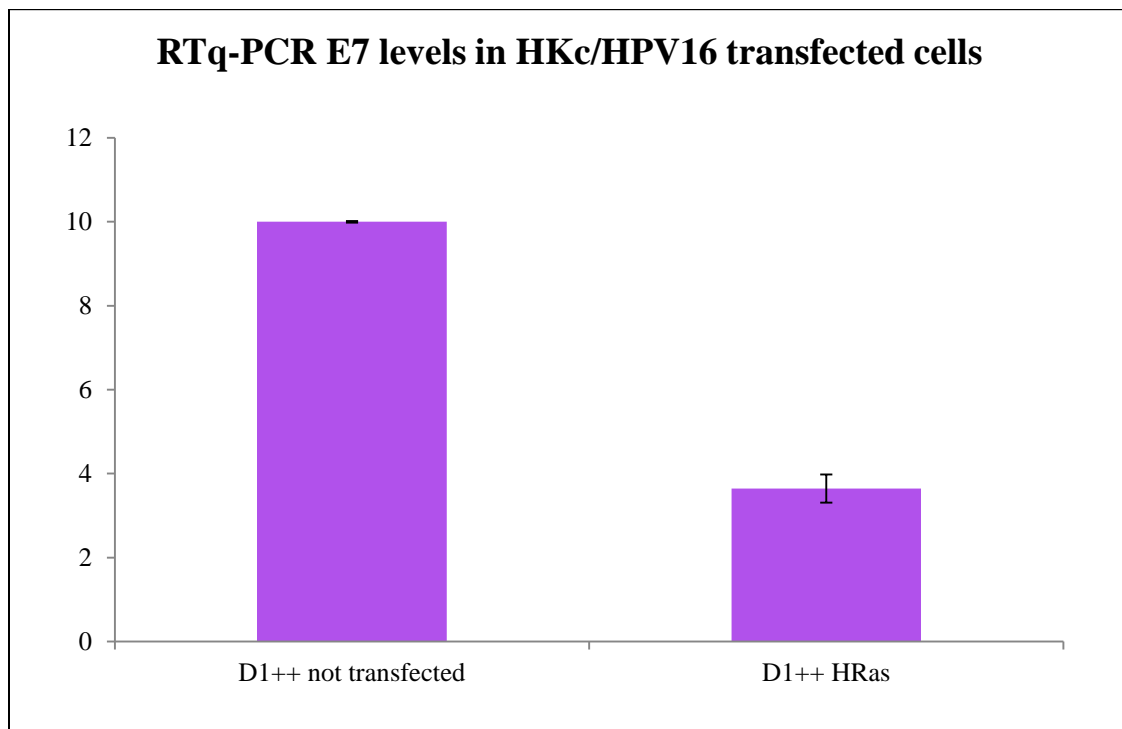


Figure 3.12: RT/q-PCR results for E7 levels HKc16/D1++ HRas transfected and non-transfected cell line.

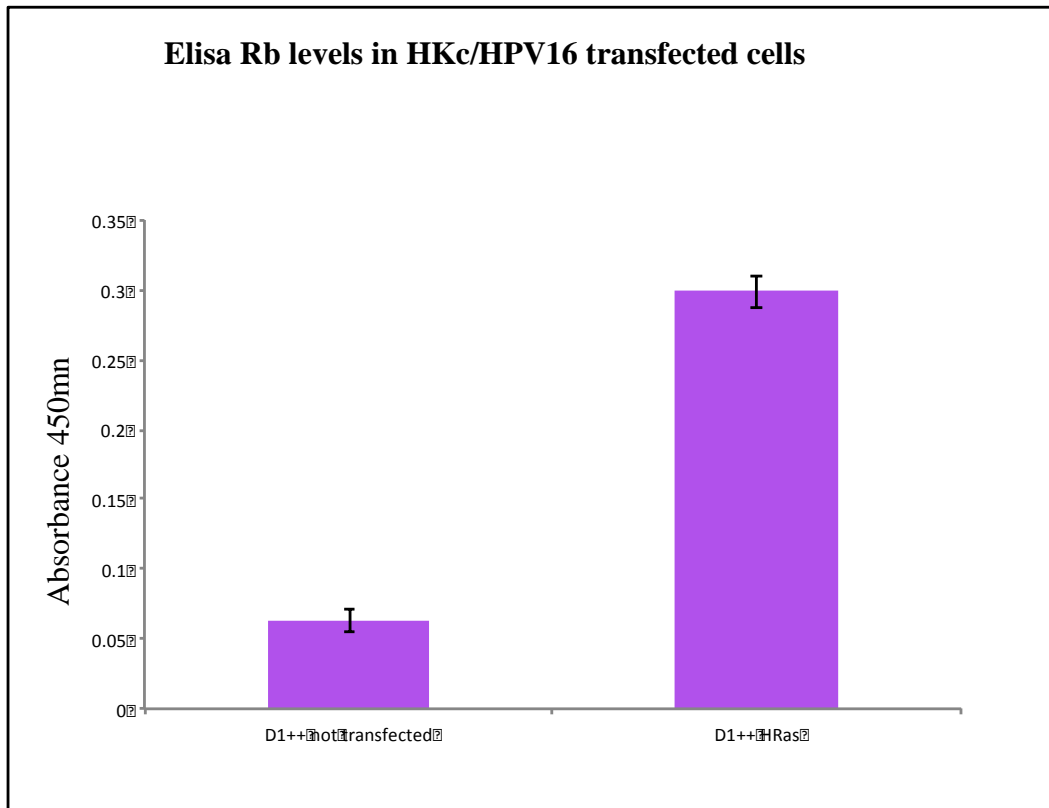


Figure 3.13. Rb levels in HKc/HPV16d-1 (D1++) cells transfected with H-Ras and their non-transfected control

3.3 Aim 2

To determine whether p53 can be knock-down by the means of an shRNA in Human Keratinocyte lines transformed with HPV16 (HKc/HPV16) and HKc/DR lines.

3.3.1 UV treatment results

First, in order for the cells to produce sufficient amount of p53 protein, normal human keratinocytes (HKc) and HKc/HPV16 were stressed using UV light in order to induce p53 protein production. The cells were given some time to recover with fresh CM medium after the UV treatment (1, 3, 6 and 12 hours). p53 protein levels were first measured via ELISA in normal (HKc) as a control. The graph below (figure 14) shows the result of p53 ELISA after UV treatment in HKc. In UV treated cells, we can make better comparisons in p53 protein levels between the following groups: HKc non-treated, HKc 1 hour after treatment and HKc 12 hours after treatment. HKc/HPV16 cell lines p53 ELISA after UV treatment graphs are also shown below (figure 15 and 16). HKc/HPV16 non-transfected cell lines, early passage number (figure 15), did not respond to UV treatment until 12 hours, where we noticed a slight increase in p53 proteins levels. However, later passage HKc/HPV16 non-transfected cell lines (Figure 16) did not have a change in p53 protein levels after UV treatment.

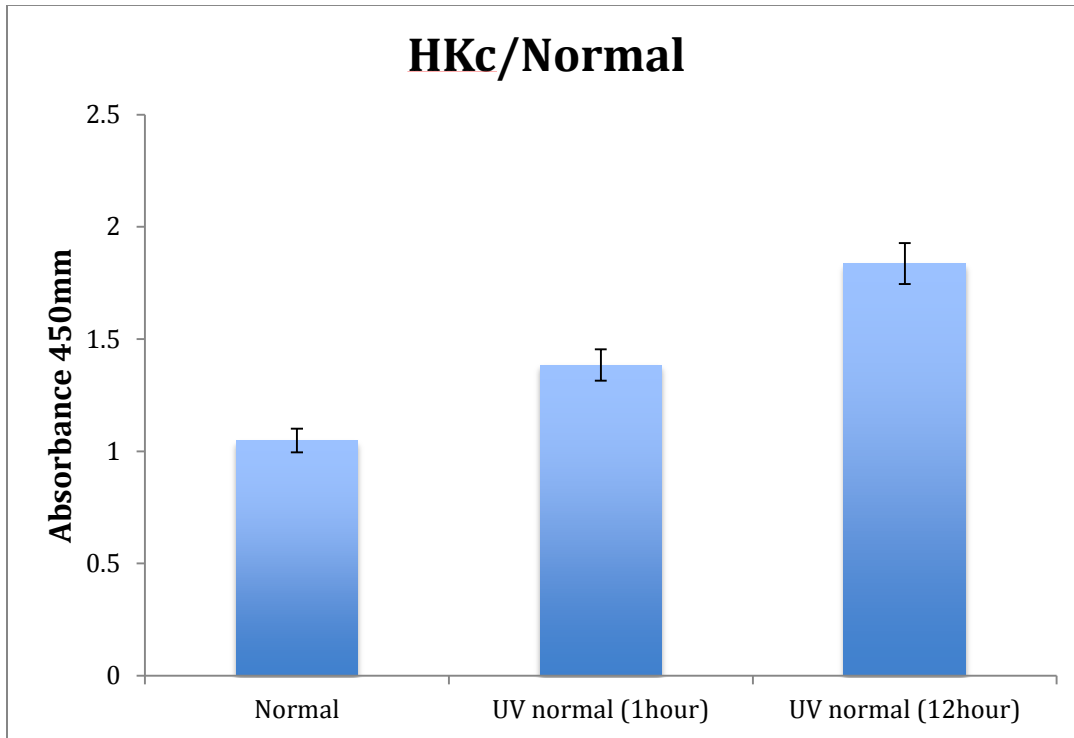


Figure 3.14. p53 ELISA results in normal HKc. P53 protein levels was shown to significantly increase after 1 and 12 hour after UV treatment as compared the non-UV treated normal.

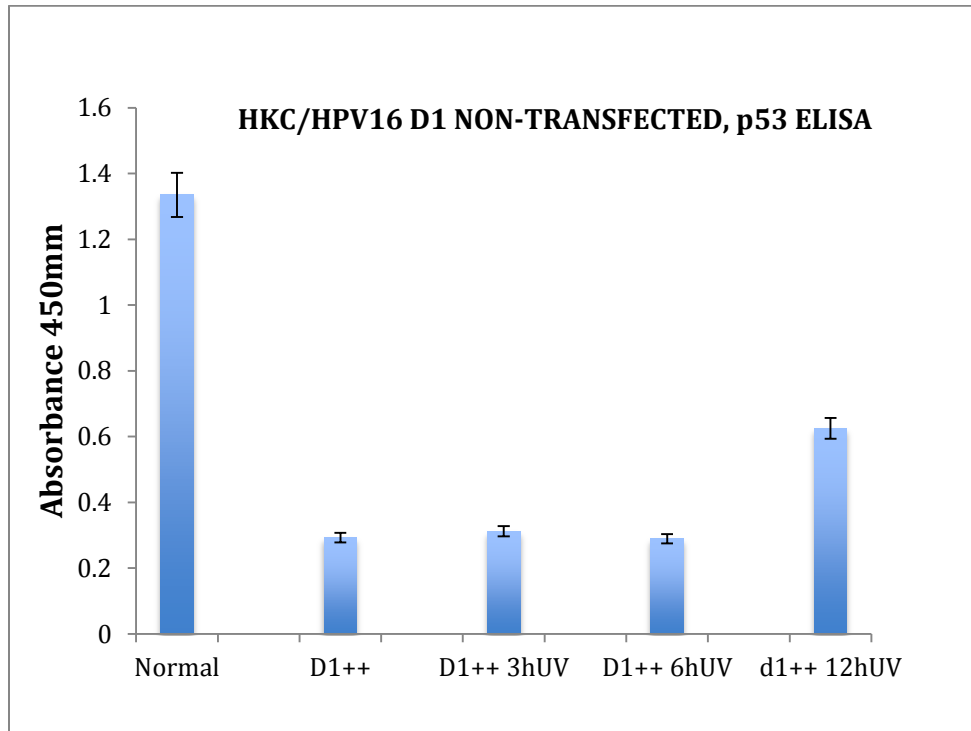


Figure 3.15. p53 ELISA results in HKc/HPV16 non-transfected UV treated cells. (Passage number: 25). A significant decrease in p53 protein levels in HKc/HPV16 (D1++) transformed cell lines was noticed as compared to a normal human keratinocytes (HKc). After UV treatment, we do not notice an increase in p53 protein levels (at 1h and 3h after UV) except after 12 hours post UV.

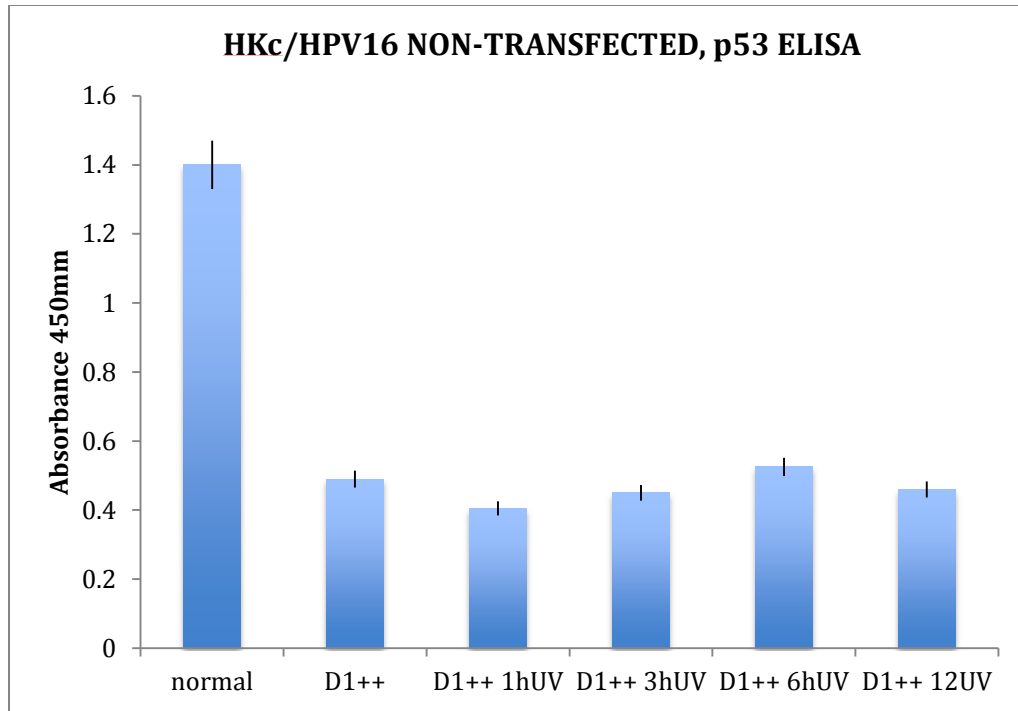


Figure 3.16. 53 ELISA results in HKc/HPV16 non-transfected UV treated cells. (Passage number: 35) Once again we notice a significant decrease in p53 protein as compared to normal Human keratinocytes (HKc/normal). However p53 protein levels stayed the same after UV treatment (1h, 3h, 6h and 12 hour after UV).

3.3.2 Human Keratinocyte lines transformed with HPV16 (HKc/HPV16) and HKc/DR lines

I wanted to determine whether p53 can be knock-down by the means of an shRNA in Human Keratinocyte lines transformed with HPV16 (HKc/HPV16) and HKc/DR lines. Therefore, I performed a p53 ELISA in our HKc/HPV16 transfected with p53i-sh cell line (and their respective controls), additionally we treated them with UV to induce p53 production. Figure 15 shows the results of a p53 ELISA comparing p53 levels in HKc/HPV16d-1 (D1++) to normal HKc and to D1++ transfected with p53shRNA. As compared to control normal HKc, the HKc/HPV16d-1 cell line expresses significantly lower level of p53 protein. In HKc/HPV16d-1 transfected with p53i-sh (D1++ non-transfected, non UV) we observe even lower p53 proteins levels. However after UV treatment, the HKc/HPV16d-1 cell lines transfected with p53i-sh still show a surprising ability to increase expression of p53, which returns to almost the same level of protein observed in our control (HKc), but does not reach the expression levels triggered by UV treatment in normal HKc.

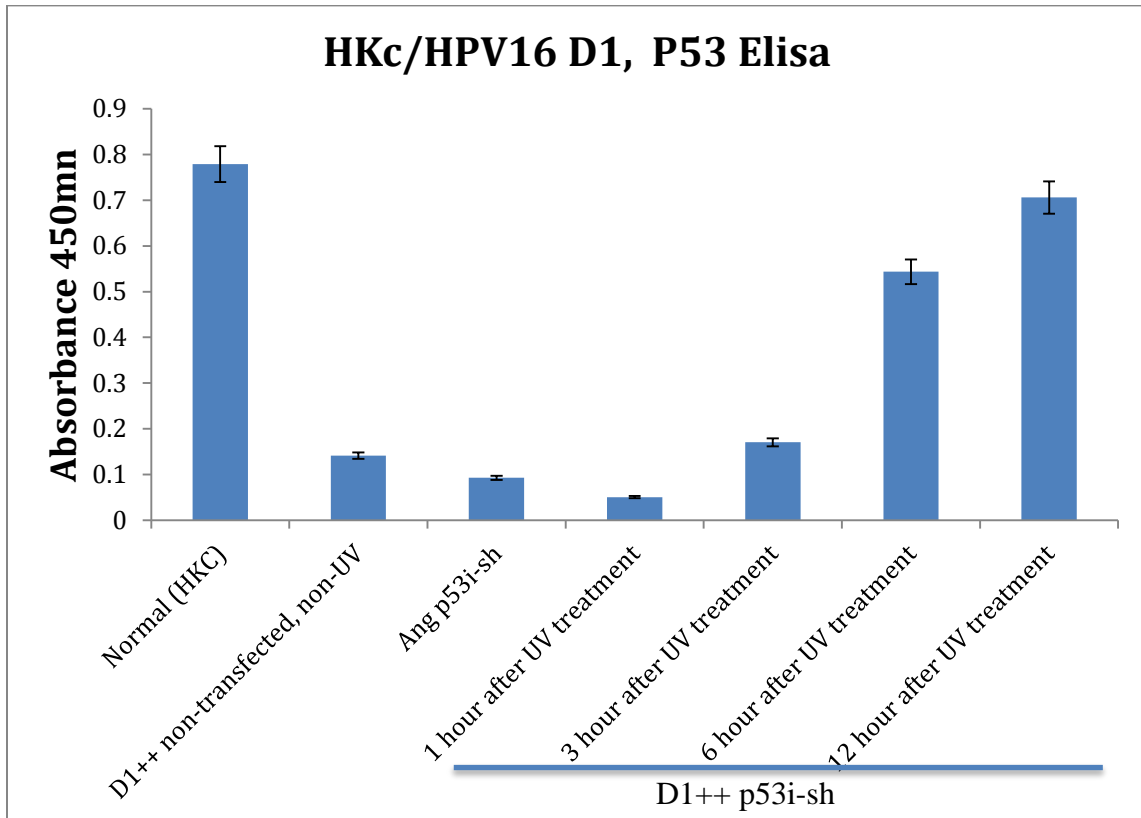


Figure 3.17. Tp53 ELISA results in the HKc/HPV16d-1 cell line (D1++). The bar graph is listed as follows (left to right) HKc (normal), HKc/HPV16 D1 (non-transfected and non-UV treated), HKc/HPV16 D1 transfected with p53i-sh (non-UV treated), HKc/HPV16 D1 transfected with p53i-sh (1hour after UV treatment), HKc/HPV16 D1 transfected with p53i-sh (3hour after UV treatment), HKc/HPV16 D1 transfected with p53i-sh (6hour after UV treatment), HKc/HPV16 D1 transfected with p53i-sh (12hour after UV treatment) respectively.

Looking at the morphology of HKc/HPV16 cells transfected with p53i-sh after UV treatment, we notice that the cells are very responsive to UV treatment, as early as 1 hour after UV.

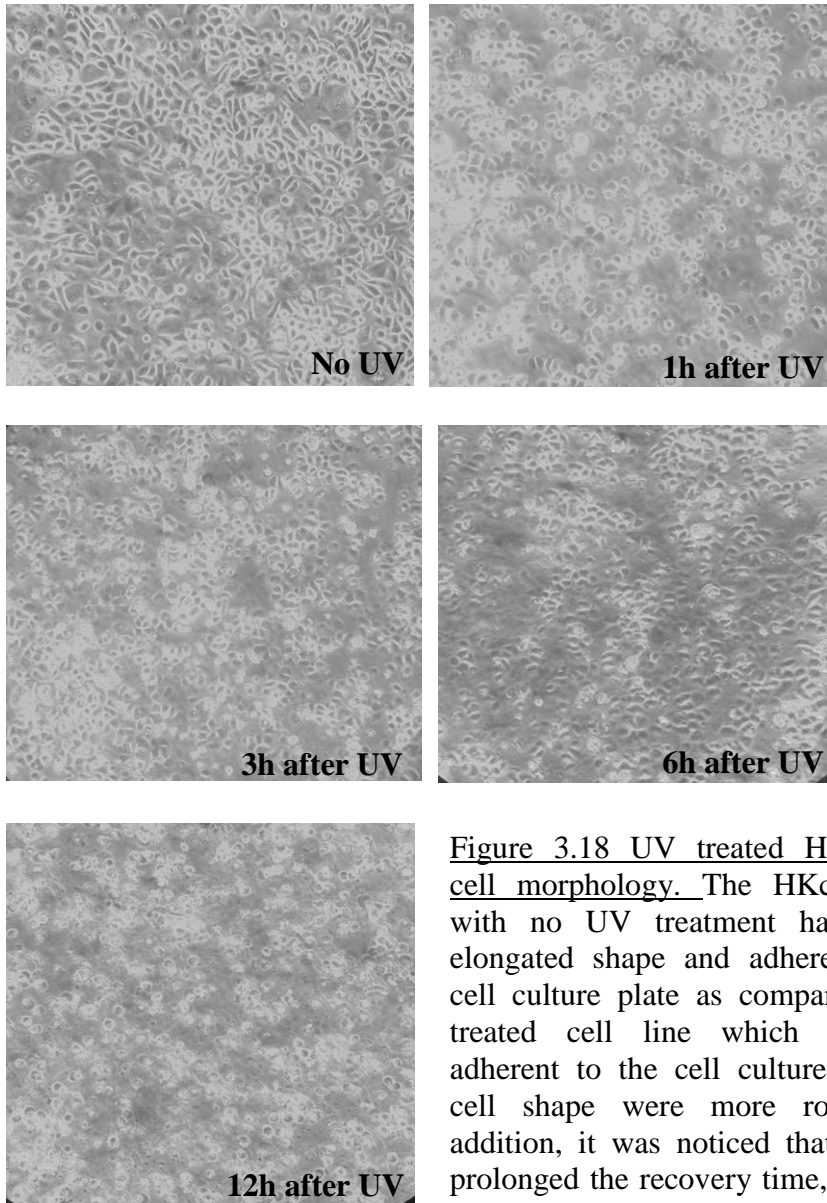


Figure 3.18 UV treated HKc/HPV16 cell morphology. The HKc cell line with no UV treatment has a more elongated shape and adhere better to cell culture plate as compared to UV treated cell line which were less adherent to the cell culture plate and cell shape were more rounded. In addition, it was noticed that the more prolonged the recovery time, the higher

Differentiation resistant (HKc/DR) cells lines were transfected with p53i-sh and UV treated. The cells were shown to have

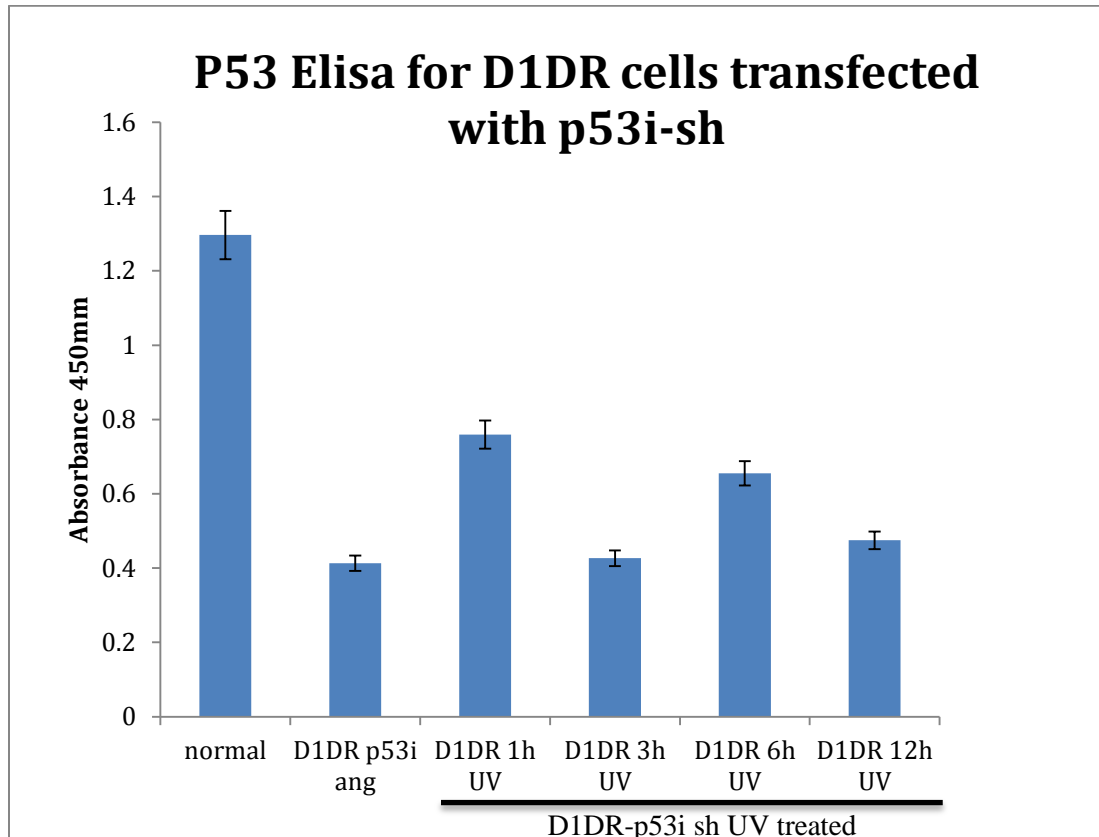


Figure 3.19. HKc/DR Similar to our HKc/HPV16 p53i-sh transfected cells line. We also notice a significant decrease in p53i protein levels in our differentiation resistant transfected cell lines as compared to our control (HKc/Normal). When UV treated, the p53 protein levels in those cell did increase, however we notice a rather an unsettle increase and decrease of p53 proteins levels in those cells after UV treatment.

Looking at the morphology of HKc/DR cells transfected with p53i-sh after UV treatment, we notice that the cells are more resistant to UV treatment. Morphological changes due to UV treatment is not noticed until 6 and 12 hour after UV.

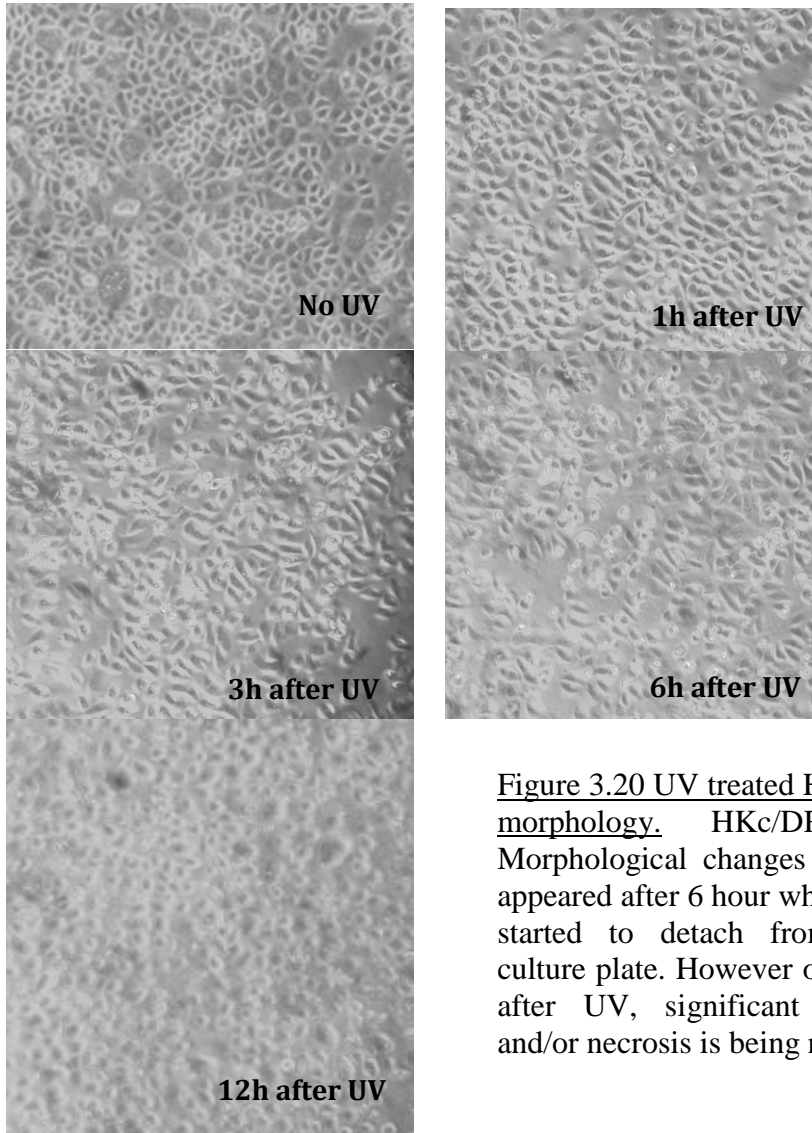


Figure 3.20 UV treated HKc/DR cell morphology. HKc/DR p53i-sh Morphological changes due to UV appeared after 6 hour where the cells started to detach from the cell culture plate. However only 12-hour after UV, significant cell death and/or necrosis is being noticed.

Furthermore, an ELISA assay was done in order to detect a difference in p53 protein levels in the HKc/HPV16 D1 transfected with mutated HRAs using the ELISA assay (Figure 22). Surprisingly, HKc/HPV16d-1 cells transfected with H-RasV12 showed lower levels of p53, as compared to their non-transfected controls. As expected, HKc/HPV16 D1 non-transfected had much lower p53 protein expression as compared to the normal (HKc).

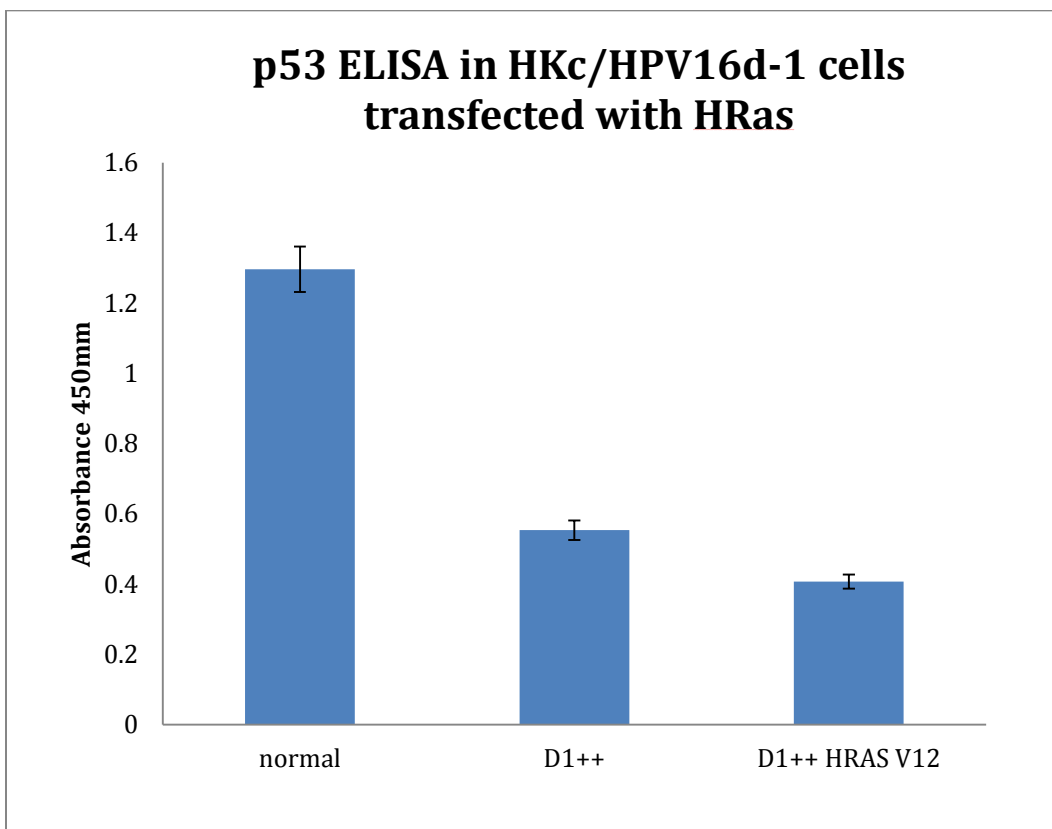


Figure 3.21. ELISA p53 levels in HKc/HPV16d-1 cells transfected with HRas.

CHAPTER 4 DISCUSSION

We noticed in the data shown above that p53 levels were at least ten-fold higher in normal HKc than in HKc/HPV16d-1 not exposed to UV. This difference is to be attributed to the fact that in HKc/HPV16, E6 promotes p53 degradation; hence the steady-state levels of p53 are much lower. Transfection with the p53shRNA plasmid decreases steady-state p53 levels even more (D1++angp53i Transfected). When treated with UV, the p53i-transfected HKc/HPV16 cells show a further decrease in p53 levels after one hour, and a delayed increase at 6 h. However, at 12 hours after UV treatment, the levels of p53 in D1++angp53i Transfected cells are still lower than those in untreated normal HKc. As shown in figure 11, HPV16 E7 mRNA levels decreased by about 2/3 in HKc/HPV16d-1 transfected with H-RasV12. This may indicate that H-RasV12 is partially “replacing” E7 function. To confirm that E7 expression was indeed decreased in these cells, we performed an ELISA for Rb. As expected, the Rb ELISA shows a marked increase in Rb protein levels in the HKc/HPV16d-1 cells transfected with H-RasV12. This indicates that E7 function is at least partially lost in these cells, and Rb is no longer being degraded or at least not to the same extent as in non-transfected HKc/HPV16d-1.

As I previously mentioned, HARasV12-transfected HKc/HPV16 express lower levels of HPV16 E7 (figure 12), and E7 function appears to be decreased as well, because Rb protein levels rise (figure 13). This finding supports the notion that E7 function may be “replaced” in HPV-transformed cells by changes in genes that support/maintain

proliferation. HKc/HPV16, and HKc/HPV16 expressing an shRNA against p53, exhibit some residual ability to respond to UV treatment with an induction of p53 (figure 18). Accordingly, UV treatment produces visible damage in these cells. HKc/DR appear to be more resistant than HKc/HPV16 to UV treatment, exhibiting only minor (if at all) increases in p53 levels. Thus, morphological evidence of cells death in UV treated HKc/DR is observed only 12h after treatment and not earlier (figure 20). These are interesting observations that warrant full characterization of the UV responses of HPV-transformed cells at early and late stages of progression. P53 levels decrease slightly in HKc/HPV16 transfected with HRasV12(figure 21): this could be due to the decrease of E7 levels and activity, as E7 is known to stabilize p53. More work is needed to determine the levels of E6 and E7 in p53shRNA-expressing HKc/HPV16 and HKc/DR, to conclusively provide proof of principle for our hypothesis

Future Work

The results shown above are encouraging. However, we need to demonstrate positively that H-Ras is expressed in the transfected cells, and also investigate how H-Ras cells grow: we have observed slower growth in H-RasV12-transfected cells than in their parental cell line, but we need to actually measure their growth rate. We presume that the decrease in E7 mRNA expression would be accompanied by a decrease in E6, as E6 and E7 messages derive from the same polycistronic mRNA, and in order to produce E7 cells must splice out most of E6. With less E6, there is more p53 to go around, and cells are known to respond to mutated Ras by increasing p53 levels and arresting growth. We

presume that this may be the mechanism that slows down growth in H-RasV12-transfected cells, but we need to demonstrate that this is (or is not) the case.

Additionally, we should assess the effects of the combined expression of p53 shRNA and H-RasV12 on E6/E7 expression in HKc/HPV16 and HKc/DR lines by co-transfection of p53 and H-RasV12 in HKc/HPV16 cells lines. Using this approach will help us to assess if HKc/HPV16 and HKc/DR lines can become more independent on E6/E7 activities for proliferation. Additional efforts should be dedicated to exploring the mechanisms by which HRas signaling leads to decreased expression of E7 in HKc/HPV16, as well as, exploring the effects of knocking out p53 using CRISPR instead of shRNA.

REFERENCES

1. Jemal A, Bray F, Center MM, Ferlay J, Ward E, Forman D. Global cancer statistics. *CA Cancer J Clin* 2011;61:69–90.
2. Curado MP, Boyle P. Epidemiology of head and neck squamous cell carcinoma not related to tobacco or alcohol. *Curr Opin Oncol* 2013;25:229–34.
3. Smith EM, Ritchie JM, Summersgill KF, Hoffman HT, Wang DH, Haugen TH, Turek LP. Human Papillomavirus in Oral Exfoliated Cells and Risk of Head and Neck Cancer. *JNCI J Natl Cancer Inst* 2004;96:449–55.
4. Malloy KM, Ellender SM, Goldenberg D, Dolan RW. A survey of current practices, attitudes, and knowledge regarding human papillomavirus-related cancers and vaccines among head and neck surgeons. *JAMA OtolaryngologyHead & Neck Surg* 2013;139(10):1037–42
5. Ramqvist T, Dalianis T. Oropharyngeal cancer epidemic and human papillomavirus. *Emerg Infect Dis* 2010;16:1671–7.
6. Bouvard V, Baan R, Straif K, Grosse Y, Secretan B, Ghissassi F El, Benbrahim-Tallaa L, Guha N, Freeman C, Galichet L, Coglianò V. A review of human carcinogens—Part B: biological agents. *Lancet Oncol* 2009;10:321–2.
7. Boscolo-Rizzo P, Del Mistro A, Bussu F, Lupato V, Baboci L, Almadori G, DA Mosto MC, Paludetti G. New insights into human papillomavirus-associated head and neck squamous cell carcinoma. *Acta Otorhinolaryngol Ital* 2013;33:77–87.

8. Braakhuis BJM, Brakenhoff RH, Meijer CJLM, Snijders PJF, Leemans CR. Human papilloma virus in head and neck cancer: the need for a standardised assay to assess the full clinical importance. *Eur J Cancer* 2009;45:2935–9.
9. Nichols AC, Dhaliwal SS, Palma D a, Basmaji J, Chapeskie C, Dowthwaite S, Franklin JH, Fung K, Kwan K, Wehrli B, Howlett C, Siddiqui I, et al. Does HPV type affect outcome in oropharyngeal cancer? *J Otolaryngol Head Neck Surg* 2013;42:9.
10. Bernard H-U, Burk RD, Chen Z, van Doorslaer K, zur Hausen H, de Villiers E-M. Classification of papillomaviruses (PVs) based on 189 PV types and proposal of taxonomic amendments. *Virology* 2010;401:70–9.
11. Favre M. Structural polypeptides of rabbit, bovine, and human papillomaviruses. *J Virol* 1975;15:1239–47.
12. De Villiers E-M, Fauquet C, Broker TR, Bernard H-U, zur Hausen H. Classification of papillomaviruses. *Virology* 2004;324:17–27.
13. Bienkowska-Haba M, Sapp M. The cytoskeleton in papillomavirus infection. *Viruses* 2011;3:260–71.
14. Walboomers JM, Jacobs MV, Manos MM, Bosch FX, Kummer JA, Shah KV, Snijders PJ, Peto J, Meijer CJ, Muñoz N; Jacobs; Manos; Bosch; Kummer; Shah; Snijders; Peto; Meijer; Muñoz (1999). "Human papillomavirus is a necessary cause of invasive cervical cancer worldwide". *J. Pathol.* 189 (1): 12–9. doi:10.1002/(SICI)1096-9896(199909)189:1<12::AID-PATH431>3.0.CO;2-F. PMID 10451482.
15. Cardesa A, Nadal A. Carcinoma of the head and neck in the HPV era. *Acta Dermatovenerol Alp Panonica Adriat* 2011;20:161–73.

16. De Villiers E-M. Cross-roads in the classification of papillomaviruses. *Virology* 2013;
17. Levine AJ¹, Oren M. The first 30 years of p53: growing ever more complex. *Nat Rev Cancer*. 2009 Oct;9(10):749-58. doi: 10.1038/nrc2723
18. Rotgers E¹, Rivero-Müller A², Nurmio M¹, Parvinen M², Guillou F³, Huhtaniemi I⁴, Kotaja N², Bourguiba-Hachemi S⁵, Toppari J¹. Retinoblastoma protein (RB) interacts with E2F3 to control terminal differentiation of Sertoli cells. *Cell Death Dis*. 2014 Jun 5;5:e1274. doi: 10.1038/cddis.2014.232.
19. Howie HL, Katzenellenbogen RA, Galloway DA. Papillomavirus E6 proteins. *Virology* 2009;384:324–34.
20. McLaughlin-Drubin ME, Münger K. The human papillomavirus E7 oncoprotein. *Virology* 2009;384:335–44.
21. Baker CC, Phelps WC, Lindgren V, Braun MJ, Gonda MA, Howley PM. Structural and transcriptional analysis of human papillomavirus type 16 sequences in cervical carcinoma cell lines. *J Virol* 1987;61:962–71.
22. Schwarz E, Freese UK, Gissmann L, Mayer W, Roggenbuck B, Stremlau A, zur Hausen H. Structure and transcription of human papillomavirus sequences in cervical carcinoma cells. *Nature* 1985;314:111–4.
23. Gage JR, Meyers C, Wettstein FO. The E7 proteins of the nononcogenic human papillomavirus type 6b (HPV-6b) and of the oncogenic HPV-16 differ in retinoblastoma protein binding and other properties. *J Virol* 1990;64:723–30.
24. Münger K, Werness BA, Dyson N, Phelps WC, Harlow E, Howley PM. Complex formation of human papillomavirus E7 proteins with the retinoblastoma tumor suppressor gene product. *EMBO J* 1989;8:4099–105.

25. Scheffner M, Werness BA, Huibregtse JM, Levine AJ, Howley PM. The E6 oncoprotein encoded by human papillomavirus types 16 and 18 promotes the degradation of p53. *Cell* 1990;63:1129–36.
26. Dyson N, Howley PM, Münger K, Harlow E. The human papilloma virus-16 E7 oncoprotein is able to bind to the retinoblastoma gene product. *Science* 1989;243:934–7.
27. Münger K, Baldwin A, Edwards KM, Hayakawa H, Nguyen CL, Owens M, Grace M, Huh K. Mechanisms of human papillomavirus-induced oncogenesis. *J Virol* 2004;78:11451–60. 122
28. Moody C a, Laimins L a. Human papillomavirus oncoproteins: pathways to transformation. *Nat Rev Cancer* 2010;10:550–60.
29. Vogelstein B, Lane D, Levine AJ. Surfing the p53 network. *Nature* 2000; 408: 307–310.
30. Kandoth C, McLellan MD, Vandin F, Ye K, Niu B, Lu C *et al.* Mutational landscape and significance across 12 major cancer types. *Nature* 2013; 502: 333–339
31. Agrawal N, Frederick MJ, Pickering CR, Bettegowda C, Chang K, Li RJ *et al.* Exome sequencing of head and neck squamous cell carcinoma reveals inactivating mutations in NOTCH1. *Science* 2011; 333: 1154–1157.
32. Stransky N, Egloff AM, Tward AD, Kostic AD, Cibulskis K, Sivachenko A *et al.* The mutational landscape of head and neck squamous cell carcinoma. *Science* 2011; 333: 1157–1160
33. Nature. 2015 Jan 29;517(7536):576-82. doi: 10.1038/nature14129.

34. Pylayeva-Gupta, Y., Grabocka, E. & Bar-Sagi, D. RAS oncogenes: weaving a tumorigenic web. *Nat. Rev. Cancer* 11, 761–774 (2011)
35. Rampias T, Giagini A, Siolos S, Matsuzaki H, Sasaki C, Scorilas A, Psyrri A². RAS/PI3K crosstalk and cetuximab resistance in head and neck squamous cell carcinoma. *Clin Cancer Res.* 2014 Jun 1;20(11):2933-46.
36. Weinberger et al. Characterization of HPV and host genome interactions in primary head and neck cancers. *Proc Natl Acad Sci U S A.* 2014 Oct 28;111(43):15544-9. doi: 10.1073/pnas.1416074111. Epub 2014 Oct 13.
37. Tomar, S. Differential Gene Expression Pattern in HPV-positive and HPV-negative Oropharyngeal Carcinoma. (Doctoral thesis). Retrieved from ProQuest Dissertations and Theses.